Contents lists available at ScienceDirect

Spatial Statistics

journal homepage: www.elsevier.com/locate/spasta

A spatial model with vaccinations for COVID-19 in South Africa

Claudia Dresselhaus [a], Inger Fabris-Rotelli [a,*], Raeesa Manjoo-Docrat [c],
Warren Brettenny [e], Jenny Holloway [b], Nada Abdelatif [d], Renate Thiede [a],
Pravesh Debba [b], Nontembeko Dudeni-Tlhone [b]

[a] *Department of Statistics, University of Pretoria, South Africa*
[b] *Council for Scientific and Industrial Research, South Africa*
[c] *Department of Statistics and Actuarial Science, University of Witwatersrand, South Africa*
[d] *Biostatistics Research Unit, South African Medical Research Council, South Africa*
[e] *Department of Statistics, Nelson Mandela University, South Africa*

ARTICLE INFO

ABSTRACT

Since the emergence of the novel COVID-19 virus pandemic in December 2019, numerous mathematical models were published to assess the transmission dynamics of the disease, predict its future course, and evaluate the impact of different control measures. The simplest models make the basic assumptions that individuals are perfectly and evenly mixed and have the same social structures. Such assumptions become problematic for large developing countries that aggregate heterogeneous COVID-19 outbreaks in local areas. Thus, this paper proposes a spatial SEIRDV model that includes spatial vaccination coverage, spatial vulnerability, and level of mobility, to take into account the spatial–temporal clustering pattern of COVID-19 cases. The conclusion of this study is that immunity, government interventions, infectiousness and virulence are the main drivers of the spread of COVID-19. These factors should be taken into consideration when scientists, public policy makers and other stakeholders in the health community analyse, create and project future disease prevention scenarios. Such a model has a place for disease outbreaks that may occur in future, allowing for the inclusion of vaccination rates in a spatial manner.

1. Introduction

Since the emergence of the novel COVID-19 virus pandemic in December 2019, numerous mathematical models were published to assess the transmission dynamics of the disease, predict its future course, and evaluate the impact of different control measures. The reviews Shankar et al. (2021), Gnanvi et al. (2021), Kong et al. (2022) report that the Susceptible–Exposed–Infected–Recovered (SEIR) compartmental model is a popular epidemiological model. The majority of modellers used compartmental models (SEIR-type models) for predicting the spread of a disease. These models are well-known for being able to take the dynamics of spread into account, by utilising a set of differential equations (Kong et al., 2022). These differential equations can be adapted to include numerous parameter estimates affecting spread, such as vaccinations, hospitalisation and other interventions (Gnanvi et al., 2021). In circumstances, where the data availability is scarce and the intervention planning requires a great deal of detail, SEIR-type models become favourable (Silal et al., 2022; Whitty, 2015; Adam, 2020). This is because they are good at predicting worst-case scenarios and can estimate the impact of interventions with a combination of expert advice and limited data (Shankar et al., 2021).

---

* Corresponding author.
  E-mail address: inger.fabris-rotelli@up.ac.za (I. Fabris-Rotelli).

Many of these SEIR models use the basic reproduction number (R_0). This parameter is of particular importance as R_0 estimates the speed at which a disease is capable of spreading in a population (Cheng et al., 2020; Dhirasakdanon and Thieme, 2009; Park et al., 2020). R_0 refers to the average number of secondary infections caused by a single infectious individual introduced into a completely susceptible population (Anderson and May, 1985). For SARS-COV-2, the R_0 value for the various provinces in South Africa was estimated at 1.7 to 2.5, according to the NICD (Cohen, 2020). This means that one infected person will on average infect 1.7 to 2.5 additional people. On the contrary, the effective reproduction number, R_e, is R_0 compromised under the influence of immunisation, vulnerability and protection measures (Locatelli et al., 2021).

The simplest SEIR models make the basic assumptions that everyone has an equal chance to be exposed to an infected person, because the population is homogeneous (Adam, 2020). A population is said to be homogeneous if the social structure is the same and individuals are perfectly and evenly mixed (Diggle, 2006). This assumption becomes problematic for large countries that aggregate heterogeneous COVID-19 outbreaks in local areas (Jewell et al., 2020). Local predictions are therefore necessary to adequately assess the spatial–temporal clustering pattern of COVID-19 cases (Huang et al., 2020; Ma et al., 2021) in a large and diverse country such as South Africa.

South Africa has deep-rooted inequalities causing stark differences in access to basic municipal services such as health care, running water, sanitation, housing and social amenities (Jalilisadrabad and Zabetian Targhi, 2020). The historical spatial planning of the colonial and apartheid system has had the most profound influence on the cities that exist in South Africa (Jalilisadrabad and Zabetian Targhi, 2020). Apartheid's fragmented spatial planning was used as an instrument to place discriminated people in townships on the outskirts of cities (Jalilisadrabad and Zabetian Targhi, 2020). The past policies of spatial segregation have left a legacy of poverty and inequality, which are reflected in poor communities located in former homelands and townships (Turok et al., 2021). Considering South Africa's spatial segregation, the COVID-19 epidemic did not take the same course in all areas of South Africa, even when important factors such as age distribution are considered (Adam, 2020). To understand better the risks COVID-19 poses to vulnerable communities, the National Disaster Management Centre, together with the Council of Scientific and Industrial Research, built the COVID-19 Vulnerability Dashboard.[1]

Even though South Africa introduced a strict lockdown at the onset of the COVID-19 pandemic, impoverished individuals continued to travel from settlements into the cities during this time, due to many living day-to-day for food. The effect of former Apartheid policies and the ensuing formation of townships and consequent movement, mainly with minibus taxis, from townships to suburbs and to the centre of towns will inevitably determine mobility and movement patterns (Woolf and Joubert, 2013, 2014). This mobility is reflected in the mobility data available for this research.[2] Including mobility rates in the prediction model is therefore an important factor in South Africa, even under lockdown measures (Potgieter et al., 2021).

The climate crisis in the 21st century, together with agricultural land use, livestock farming, and urbanisation are changing the habitats of pathogens (Smit et al., 2020). High contact between humans and animals through breeding, hunting, as well as trade in exotic delicacies increases the risk of spreading zoonotic disease to humans. An example of a zoonotic disease is Influenza (flu) Type A, which is a respiratory infection in mammals and birds (Baigent and McCauley, 2003).

During the COVID-19 pandemic, early studies focused on tracking the pandemic rather than implementing vaccinations spatially (Fry et al., 2021; Auchincloss et al., 2012). Specifically, since vaccinations are seen as an effective way to reduce morbidity and mortality in the COVID-19 pandemic (World Health Organisation, 2023), an influx of works that introduced models which contribute to the understanding of the impact of vaccination was observed (Feng et al., 2011; Wang et al., 2020). Typically location, time, and to whom the vaccination should be provided were dimensions used to evaluate vaccination allocation strategies (Hafeez et al., 2020). Ignoring these spatiotemporal dimensions may lead to an inefficient vaccination distribution strategy (Zhou et al., 2021). Incorporating the vaccination compartment gives valuable insight by simulating various vaccine distributions scenarios and choosing the vaccine policies that minimises the death toll of a vaccine preventable disease (Ben Chaouch et al., 2022; Silal et al., 2020; Silal, 2022).

Some studies do however incorporate spatio-temporal information, such as mobility predictions based on social media interactions and mobile phone networks (Zhou et al., 2021; Silal, 2022; Ben Chaouch et al., 2022; Modisenyane et al., 2022). These measures are able to provide important information about the movements of individuals and the social interactions between them. Others such as González and Villena (2020) argue that the use of simple SIRS-V type models are too simple to capture the complexities of human interactions, and would often incorrectly predict infection numbers. They further argue that social interactions are more prevalent between individuals in certain age groups. This implies that age-related factors are also significant in modelling the spread of diseases (Metcalf et al., 2015). Work done by Aràndiga et al. (2020) use age and mobility as features in their model, but reason differently to that of a SIRS-V model. They assume that the removed compartment is a mixture between recovered (R), vaccinated (V) or deceased (D) individuals (SEIRVD). Since vaccinated and recovered individuals are considered removed from the study, this approach assumes that vaccinated and recovered individuals will be permanently immune against the COVID-19 disease. The complexity of COVID-19 indicates both recovered and vaccinated individuals can be reinfected with COVID-19 (Kumar et al., 2021).

In Fabris-Rotelli et al. (2022), the heterogeneity in COVID-19 prevalence and its transmission rate in South Africa, as a whole, was found to be higher than in localised areas of South Africa and hence R_0 is considered to be heterogeneous spatially in South Africa (Thiede et al., 2020). To establish the variation in symptom levels and transmission rates in regions or areas, Fabris-Rotelli et al. (2022) used a spatial model to estimate the spatial spread of COVID-19. The model included vulnerability patterns in South

---

[1] Council of Scientific and Industrial Research. COVID-19 Vulnerability Dashboard, 2020. URL https://bit.ly/3iFU4Zo. (Accessed on 2020-07-09)

[2] https://data.humdata.org/dataset/movement-range-maps/ (Accessed October 2022)
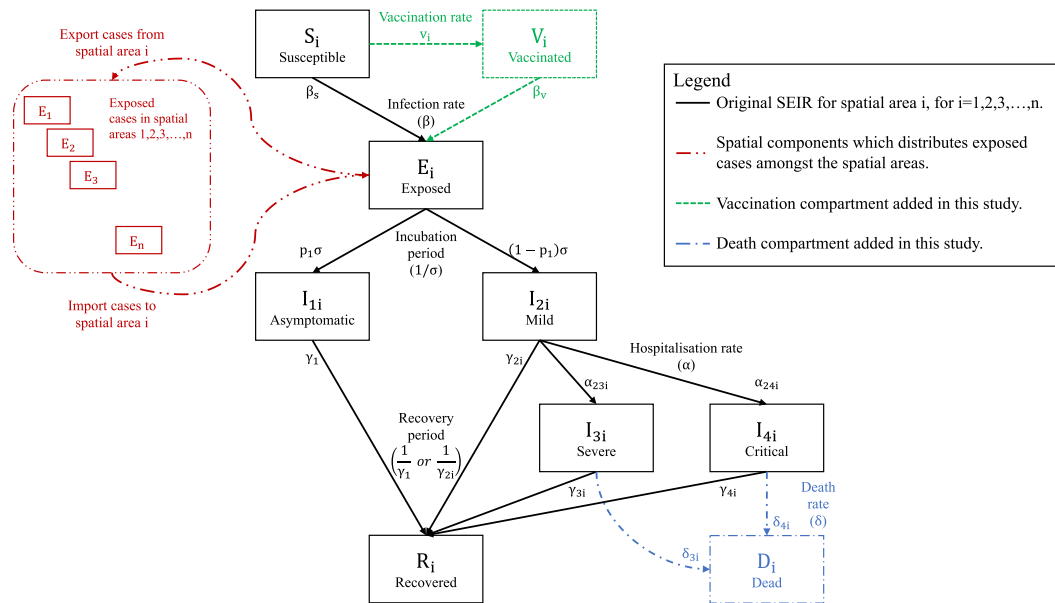
Fig. 1. The extended spatial SEIRDV model indicating the movement of exposed between spatial areas, for areas $i = 1, 2, 3, \ldots, n$.

Africa through the use of a vulnerability index per area, based on the socioeconomic and health susceptibility characteristics of each area. These indexes were produced in le Roux et al. (2021). The spatial perspective was further enriched in Fabris-Rotelli et al. (2022) with mobility patterns between spatial areas. The mobility patterns between areas are described in Potgieter et al. (2021). One aspect that Fabris-Rotelli et al. (2022) did not address is the status of immunity in an area or region, following adjustments for vulnerability and mobility. Hence the current spatial model, as described in Fabris-Rotelli et al. (2022), allows for the extension to include this aspect.

This study extends the SEIR model in Fabris-Rotelli et al. (2022) by including a vaccination compartment. Extending the model with a vaccination compartment for given areas improves the validity and accuracy of the model. A sensitivity study is conducted to analyse the results of the new model in terms of validity, reliability and accuracy. Section 2 introduces the spatial SEIRDV model, Section 3 provides the sensitivity study, Section 4 evaluates the proposed model and Section 5 concludes. All code for this work is available on a Github.[3]

It is important to mention the South African National COVID-19 Epi-Model (NCEM), which is the model by the South African COVID-19 Modelling Consortium (Silal et al., 2023). Specifically, the NCEM v2.0 district model comprehensively models COVID-19 spread for all districts of South Africa (Silal, 2022). Our model, however, is simpler and allows for incorporation of data easily accessible. Of course, with more detailed data available, our model could be expanded to additional compartments. This data was not accessible to us. An additional contribution of our model is how the mobility is modelled (Fabris-Rotelli et al., 2022), since the cellular mobility data available in Fabris-Rotelli et al. (2022) does not extend past 2020.

2. Methodology

The "Spatial Model for COVID-19 in South Africa" (Fabris-Rotelli et al., 2022) is a SEIR model, that includes spatial weight matrices determined using the methodology in Potgieter et al. (2021). The spatial weight matrices are used in the exposed compartment to imitate the movement of individuals from one geographical area to the next. Further, le Roux et al. (2021) showed that vulnerability in South Africa differs across spatial areas in terms of socioeconomic and health susceptibility characteristics. Therefore, Fabris-Rotelli et al. (2022) incorporated vulnerability levels that prove to be significantly different across spatial areas. It is important to note that the model was defined at the beginning of the pandemic, when COVID-19 vaccinations were not yet available in South Africa and not considered. Since COVID-19 vaccinations have been available since February 2021, this study aims to add a vaccination compartment to the SEIR model.

Herein, we propose the spatial SEIRDV model as displayed in Fig. 1. The proposed model consists of nine compartments namely Susceptible, Vaccinated, Exposed, Asymptomatic, Mild, Severe, Critical, Recovered and Dead.

---

[3] https://github.com/ItsClaudiPie/SEIRDV_model

2.1. Vaccination and susceptible compartments

The daily vaccination rate is indicated by v_i, that is written above the green solid line in Fig. 1. This vaccination rate depends on i and differs from wave to wave. Depending on the COVID-19 vaccine type, most individuals either need 1 or 2 dosages. In general, an individual on average receives about $E[d]$ dosages and is defined in (1).

$$E[d] = 1P[d = 1] + 2P[d = 2] \tag{1}$$

where $P[d = 1]$ or $P[d = 2]$ as the overall numerical proportion of the administered vaccine dosages in a country, encompassing both single-dose ($P[d = 1]$) and double-dose ($P[d = 2]$) proportions. This simplification is necessary when the specific breakdown of received vaccine dosages is only accessible in terms of proportions.

Using $E[d]$, we can estimate the expected number of individuals that are fully vaccinated per week for i. The estimated weekly number of fully vaccinated individuals in a spatial area i is given in Eq. (2).

$$V_i^w = \frac{doses_i^w}{E[d]} \tag{2}$$

where $doses_i^w$ is the number of weekly administered dosages for spatial area i for a given wave. The vaccination rate for a district, v_i, is calculated using Eq. (4). To estimate the daily number of fully vaccinated individuals, we divide V_i^w by the total number of days in a week. This is shown in Eq. (3)

$$V_i = \frac{V_i^w}{7} \tag{3}$$

We estimate the daily vaccination rate, which is the transition rate from the susceptible to vaccinated compartment using Eq. (4).

$$v_i = \frac{V_i}{S_i} \tag{4}$$

The rates of transition from the vaccinated or susceptible compartments to the exposed compartment are called the infection transition rates. These rates are discussed in more detail in the remainder of this subsection.

2.2. Spatial weight matrices

Potgieter et al. (2021) discuss four methods to construct spatial weight matrices. The fourth method was chosen due to the data available only from Facebook.[4] This data was used to create a so-called spatial weight matrix. Simply put, the spatial weight matrix used is a $n \times n$ matrix, which is constructed in such a way so that it quantifies w_{ij} as the amount of spatial influence that spatial area i exerts on spatial area j. The entries of the spatial weight matrix are given by Eq. (5), where $F_i^{(t)}$ is the mobility of spatial unit i at time t and d_{ij} is the standardised Euclidean distance between the centroids of spatial units i and j.

$$w_{ij}^{(t)} = (1 + F_i^{(t)}) e^{(-d_{ij})} \tag{5}$$

The $n \times n$ mobility matrices are included in the exposed compartment, to simulate the spread of the virus (Fabris-Rotelli et al., 2022). This assumption is based on the COVID-19 regulations, that enforced a quarantine on individuals who tested positive against the COVID-19 virus.

2.3. System of differential equations

The course of the infection is modelled at a daily time-step with an SEIRDV compartment model to simulate the epidemiology of the disease. In other words, at each time step t for each spatial area i, the SEIRDV visualised in Fig. 1 is modelled. The black and red dashed compartments are from the SEIR model in Fabris-Rotelli et al. (2022), but the flow has been adjusted to have the severe and critical compartments flowing from the mild, rather than being a parallel process. The blue and green compartments are the compartments that are added herein.

Altogether, the population numbers of each spatial area are denoted as N_i, and calculated as $N_i = S_i + E_i + I_{1i} + I_{2i} + I_{3i} + I_{4i} + R_i + V_i + D_i$ (see Table 1).

The number of individuals in each compartment of the model is calculated for a time point t in a spatial area i, by using a set of differential equations. Simply put, the number of individuals that transitions into a compartment are additions in the associated differential equation. The number of individuals that transitions out of a compartment are removals in the associated differential equation. The system of differential equations of the model are given as follows:

$$\frac{dS_i}{dt} = -v_i S_i - \frac{\beta_{si} S_i (\rho I_{1i} + I_{2i} + I_{3i} + I_{4i})}{N_i} \tag{6}$$

$$\frac{dV_i}{dt} = v_i S_i - \frac{\beta_{vi} S_i (\rho I_{1i} + I_{2i} + I_{3i} + I_{4i})}{N_i} \tag{7}$$

---

[4] https://data.humdata.org/dataset/movement-range-maps (Accessed October 2022)

Table 1

Terminology and notation used for in the differential equations (Equations (6)–(11)) and sensitivity analysis in Fig. 2.

Name	Equation	Description
Population Number	N_i	Number of individuals in spatial area i
Susceptible Cases	S_i	Number of susceptible individuals in spatial area i
Vaccinated Cases	V_i	Number of vaccinated individuals in spatial area i
Exposed Cases	E_i	Number of exposed individuals in spatial area i
Asymptomatic Cases	I_{1i}	Number of individuals with an asymptomatic infection in spatial area i
Mild Cases	I_{2i}	Number of individuals with a mild infection in spatial area i
Severe Cases	I_{3i}	Number of infected individuals admitted into a general ward (severe cases) in spatial area i
Critical Cases	I_{4i}	Number of infected individuals in ICU (critical cases) in spatial area i
Recovered Cases	R_i	Number of recovered individuals in spatial area i
Dead Cases	D_i	Number of dead individuals in spatial area i
Initial Immunity	–	The level of protection a population has against a pathogen before being exposed to it.
Basic Reproduction Number (R_0)	R_0	The average number that estimates the speed at which a disease is capable of spreading in a population. This parameter is influenced by factors such as the pathogen's infectiousness and the susceptibility of the population (Cheng et al., 2020; Dhirasakdanon and Thieme, 2009; Park et al., 2020).
Lockdown Scaling	$\kappa,$	The effect of the government intervention aimed at limiting human interactions during a pandemic, such as physical distancing, mask-wearing, and restrictions on gatherings, in response to the spread of the disease (Fabris-Rotelli et al., 2022).
Percentage Asymptomatic Cases	ρ	The proportion of individuals infected with a pathogen who do not show symptoms of the disease. This parameter is important for understanding the true extent of infection and can influence disease control strategies.
Mild Hospitalisation Rate	α_{23i}	The proportion of individuals infected with a pathogen who require hospitalisation and do not need intensive care. It represents the burden on healthcare systems for cases that are not severe
Mobility Rate	$w_{ij}^{(t)}$	The degree to which exposed individuals travel between spatial areas, based on (Potgieter et al., 2021).
Vulnerability	ψ_i	The vulnerability index, based on the weighted average of the normalised vulnerability indices described in le Roux et al. (2021).
Hospitalised ICU Rate	α_{24i}	The proportion of individuals infected with a pathogen who require hospitalisation and intensive care.
Incubation Period	$1/\sigma$	The time between exposure to a pathogen and the onset of symptoms. Understanding this period is crucial for identifying and isolating cases and for disease control strategies.
Hospitalised Death Rate	$\delta_{3i} = D_{3i_{dead}}/D_{3i}$	The proportion of individuals infected with a pathogen who die while hospitalised. This parameter reflects the case fatality rate among hospitalised patients.
Infective Period	σ	The duration of time during which an infected individual can transmit a disease to others. It influences the potential for disease spread within the community.
Mild Recovery Rate	$\gamma_{2i} = 1 - \gamma_1 - \gamma_{3i} - \gamma_{4i}$	The proportion of individuals infected with a pathogen who recover from the disease without requiring hospitalisation. It indicates the likelihood of recovery for non-severe cases.
Asymptomatic Recovery Rate	γ_1	The proportion of individuals infected with a pathogen who recover from the disease without showing symptoms. Due to limited knowledge of true asymptomatic cases, data on the spatial heterogeneity of this parameter are extremely limited. Thus, this parameter is assumed aspatial.
Daily Vaccination Rate	v_i	The number of vaccine doses administered per day, as a measure of the pace of vaccination efforts.
Hospitalised Recovery Rate	$\gamma_{3i} = I_{3i_{alive}}/I_{3i}$	The proportion of hospitalised individuals infected with a pathogen who recover from the disease. This parameter reflects the likelihood of recovery for severe cases.
Initial Exposed Population	E_i starting value	The portion of the population that is susceptible to infection with a pathogen at the beginning of an outbreak.
ICU Recovery Rate	$\gamma_{4i} = I_{4i_{alive}}/I_{4i}$	The proportion of individuals infected with a pathogen in intensive care who recover. This parameter is relevant for understanding outcomes among critically ill patients.
ICU Death Rate	$\delta_{4i} = D_{4i_{dead}}/D_{4i}$	The proportion of individuals infected with a pathogen who die while in intensive care. It reflects the case fatality rate among critically ill patients.

$$\frac{dE_i}{dt} = \frac{(\beta_{vi} + \beta_{si})S_i(\rho I_{1i} + I_{2i} + I_{3i} + I_{4i})}{N_i} - \sigma E_i \tag{8}$$

$$\frac{dI_{1i}}{dt} = p_1 \sigma E_i - \gamma_1 I_{1i} \tag{9}$$

$$\frac{dI_{2i}}{dt} = (1 - p_1)\sigma E_i - \gamma_{2i} I_{2i} - \alpha_{23i} I_{2i} - \alpha_{24i} I_{2i} \tag{10}$$

$$\frac{dI_{3i}}{dt} = \alpha_{23i} I_{2i} - \gamma_{3i} I_{3i} - \delta_{3i} I_{3i} \tag{11}$$

$$\frac{dI_{4i}}{dt} = \alpha_{24i} I_{2i} - \gamma_{4i} I_{4i} - \delta_{4i} I_{4i} \tag{12}$$

$$\frac{dR_i}{dt} = \gamma_1 I_{1i} + \gamma_{2i} I_{2i} + \gamma_{3i} I_{3i} + \gamma_{4i} I_{4i} \tag{13}$$

$$\frac{dD_i}{dt} = \delta_{3i} I_{3i} + \delta_{4i} I_{4i} \tag{14}$$

The system of differential equations models the course of the infection at a daily time step t. We use the system of differential equations to model a wave of infectious disease for a spatial area i. The differential equations of the SEIRDV model are used with input parameters displayed in Table A.1 in the appendix.

2.4. Modelling a wave of an infectious disease

The following algorithm is used to simulate a COVID-19 wave in South Africa for each spatial area i using the SEIRDV model proposed, allowing for uncertainty in the parameters by drawing from an appropriate distribution. The choices made for these are those motivated in Fabris-Rotelli et al. (2022), Hindmarsh (1982).

Algorithm 1 SEIRDV algorithm to simulate a COVID-19 wave

1: Where applicable, fit distributions to the input parameters of the SEIRDV model.
2: Sample input parameters of the fitted distributions.
3: Solve the system of linear equations using a ordinary differential equations solver (Hindmarsh, 1982).
4: Repeat step 3 for T time units.
5: Repeat step $2 - 4$ for multiple seeds.
6: Compute the mean and confidence interval of the model predictions.

The SEIRDV model estimates the number of individuals in a compartment for T time points, but needs the start date of the wave as an input.

The detection of the start of a wave was carried out using the method proposed in O'Brien and Clements (2021). Using this method, an Early Warning Signal (EWS) is triggered if the standard deviation, the autocorrelation function (ACF) or the return-rate, exceed two standard deviations from their cumulative mean. This EWS detector identifies a disruption in the variability of the case numbers and uses this as an indication of an impending wave.

The EWS detector and the SEIRDV algorithm were used to estimate the start date and reproduce the actual case numbers, respectively.

3. Sensitivity analysis

A construct validity test via a sensitivity analysis is done to test the robustness and validity of the SEIRDV model output. The following list outlines the terminology used in the sensitivity analysis results, which are depicted in Fig. 2.

Algorithm 2 MC algorithm to perform a probabilistic sensitivity analysis of the SEIRDV model.

1: Assign an assumed distribution for each input variable.
2: Sample a value for each input variable using its assumed distribution.
3: Enter the sampled values into the SEIRDV model.
4: Solve the system of linear equations using an ordinary differential equations solver (Hindmarsh, 1982).
5: Repeat steps $1 - 4$ N times, using a new seed for each repeat.

The results of the sensitivity study can be seen in Fig. 2, via the correlations between the parameter of the model and its outcome. The values were obtained from the runs of the MC sensitivity analysis. The input variables are the columns of this figure and the
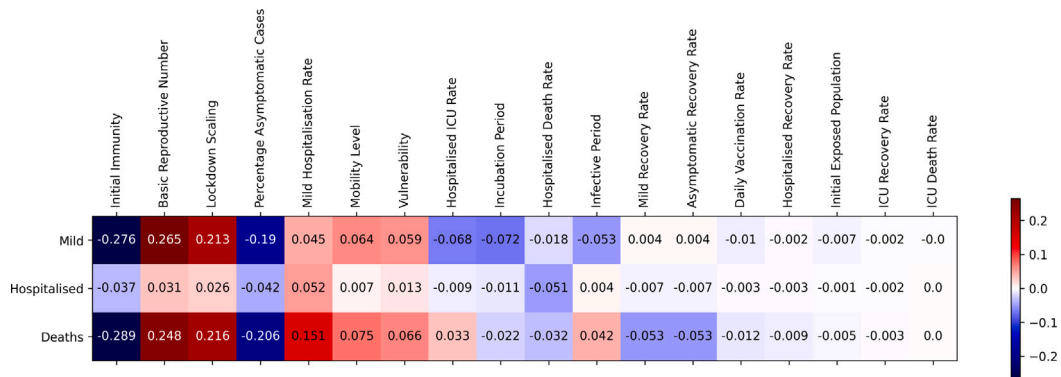
Fig. 2. Sensitivity study outcomes: positive correlation in a red scale, and negative correlation in a blue scale.

outcomes are the rows. The correlations are in ascending order, according to high positive (red) or negative (blue) correlation values. We overlay a heat-map to illustrate the correlation between SEIRDV parameters and the number of mild, hospitalised and deaths respectively. The correlation plot in Fig. 2 shows that there are strong positive and negative correlations (portrayed in vivid colours), but also weak correlations (portrayed in pale colours) for the majority of the input parameters.

The input variable that has the strongest negative correlation amongst all other variables is the vaccination level. Unmistakably, it is clear that COVID-19 cannot spread effectively if the vast majority of population is immune to it.

The correlation plot shows that the basic reproduction number and the lockdown scale have the highest positive correlation. This makes sense because an increase in R_0 increases the number of infections which, in turn, increases the number of mild, hospitalised and death cases. Similarly, the lockdown level scaling parameter κ has a positive correlation, since the higher the lockdown level scaling parameter, the more social interactions may occur and the higher the infections of COVID-19. As predicted from the literature review, if R_0 increases so does the number of infections.

In our sensitivity analyses in Fig. 2, we found that the vaccination rate, when considered within short intervals, does not have a pronounced impact on the model's outcome. Rather, it is the initial number of vaccinated individuals at the start of a given period that plays a significant role in influencing the results. This suggests that the variations in vaccination rate within these short periods do not sufficiently alter the model's projections. Hence, for the purpose of our study and to simplify the model's parameters, we chose to maintain a constant vaccination rate ν_i within each period. This decision is backed by our findings, ensuring that by setting an appropriate initial number of vaccinated individuals, our model remains robust and reflective of real-world scenarios.

Next to ν_i, the sensitivity analysis revealed that γ_1 also has no major effect on the outcome of the model. The result implies that an intricate estimation for γ_1 is not needed, and gives justice to keep γ_1 constant.

In general, transition rates show little to no effects on the number of mild, hospitalised or death cases. Since only four input variables effect the variability of the output generated by the SEIRDV model significantly, the SEIRDV model is considered robust.

4. Results

To validate whether the model can re-produce the case numbers observed, we used the estimated transition rate distributions to simulate multiple runs of the model using 50 different seeds. With the multiple runs, we obtained a confidence interval of the model's predictions. The overall runs were averaged to get the average model prediction. Based on this, we can evaluate how well the model reproduced the data that was observed. The SEIRDV algorithm to model a COVID-19 wave (Algorithm 1) is used to estimate each COVID-19 wave separately. South Africa had four significant waves of COVID-19 which can be seen in the results below.

In this application, the detection of waves was carried out for each of the 5 district municipalities in the Gauteng province using the proposed method herein. This paper focuses only on the Gauteng province, as it was significantly affected by COVID-19, due to the large population relative to the rest of the country as well as having more available data. Higher resolution data is not easily available in South Africa. The wave start dates were determined using the EWS detector.

Table 2 reports that the population numbers are larger for urban and sub-urban areas such as the City of Johannesburg, City of Tshwane and Ekurhuleni in comparison to more rural spatial areas, such as Sedibeng and West-Rand.

The calculation for the number of fully vaccinated individuals approximates the number of doses required per vaccine type, based on the number of weekly administered dosages ($doses_i^w$) and the overall numerical proportion of vaccine type given in South Africa for each wave respectively.

The approximate vaccination coverage displayed in Fig. 3 of each district is significantly greater than zero, giving reason to include vaccinations into the SEIRDV model. The vaccination coverage for City of Johannesburg and West Rand are the highest in Gauteng, whereas City of Tshwane, Ekurhuleni and Sedibeng are lower and have roughly the same vaccination coverage. Hence, it is important to adjust the model spatially to take heterogeneous vaccine coverage into account.
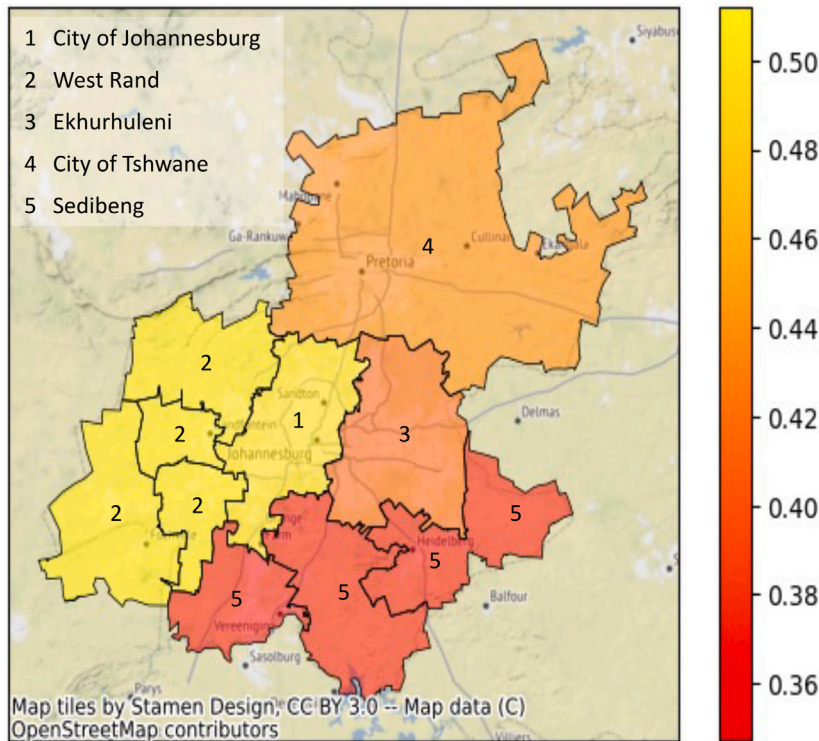
Fig. 3. A heatmap that visualises the approximate proportion of fully vaccinated individuals for each district in Gauteng (as of October 19,2022).

Table 2
Descriptive Statistics to compare the districts according to the total population numbers, the total population proportion of Gauteng, the total proportion of fully vaccinated individuals and the total proportion of tested positive cases.

Measure of comparison	City of Johannesburg	City of Tshwane	Ekurhuleni	Sedibeng	West Rand
Population number[a]	5 538 596	3 522 325	3 781 377	952 102	922 640
Population proportion of Gauteng	0.38	0.24	0.26	0.06	0.06
vaccination coverage[b]	0.41	0.36	0.33	0.29	0.43
Total proportion of tested positive cases[c]	0.07	0.07	0.05	0.07	0.06

[a] https://www.statssa.gov.za/?page_id=964 (Accessed October 2022).
[b] https://sacoronavirus.co.za/latest-vaccine-statistics (Accessed October 2022).
[c] https://www.nicd.ac.za/national-covid-19-daily-report (Accessed October 2022).

We substitute $F_i^{(t)}$ and d_{ij} in the Equation in (5). The 5 by 5 matrix consists of the estimated $w_{ij}^{(t)}$'s, which represent mobility between the 5 districts at a given day t. The daily mobility matrices are included in the exposed compartment, to simulate the spread of the virus (Fabris-Rotelli et al., 2022)

Based on the testing strategy in South Africa, where only individuals who felt sick went for testing, the assumption can be made that the detected cases would be the ones passing through the mild compartment and not the asymptomatic compartment (see Fig. 1). Fig. 4 shows the simulation study for these mild cases. The model generally over-predicts the mild cases. This is as expected, since the COVID-19 cases are typically under-reported, especially for mild cases which are not hospitalised.

Fig. 5 shows the simulation study for the hospitalised cases. The hospitalised cases are displayed as the sum of general ward cases and ICU cases. Hospitalised cases are predicted more accurately, since the confidence intervals of the model predictions capture the true observations for each wave and each district at the vast majority of given time points.

The results show that the model captures the cases well over the duration of the pandemic in South Africa, allowing for inclusion of vaccinations from the time when they were available.

5. Conclusion

The need for a model to assess the spatial–temporal clustering pattern of COVID-19 gave rise to the model developed in this paper. This study extended the spatial SEIR model developed by Fabris-Rotelli et al. (2022) to include the vaccination compartment
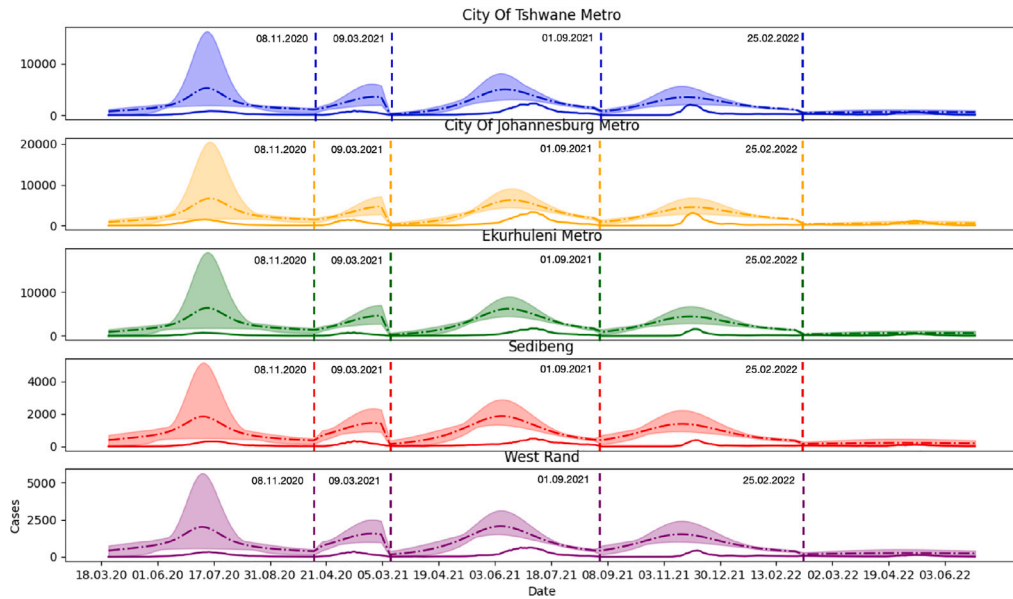
Fig. 4. Actual mild cases (solid line) vs the estimated mild cases in a (dashed line), and its confidence bounds.
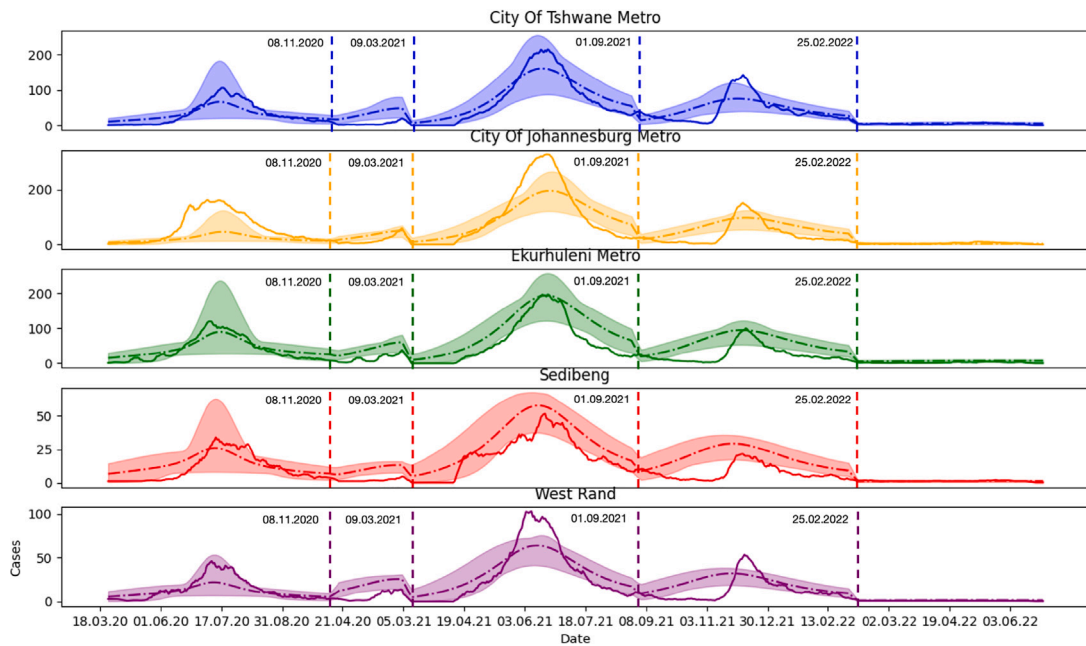

Fig. 5. Actual hospitalised cases (solid line) vs the estimated hospitalised cases in a dashed line, with confidence bounds.

to improve the validity of the model. The application focused on the districts of Gauteng. The district data was gathered from ministerial dashboards, institutes, and social media. Using data and literature, each parameter of each wave was estimated and reported in Table A.1. The SEIRDV model has a mixture of homogeneous, spatial or spatial temporal parameters. The simulation study of the spatial SEIRDV model on Gauteng data showed promising results in predicting the number of cases as well as the peak point and longevity of the wave. The primary objective was to assess whether the inclusion of a geospatially-sensitive vaccination campaign could provide better estimates of the COVID-19 pandemic in a socially heterogeneous and mobile population.

The goals of using the model to guide the government's response were met, as the model proved to fall under the responsible artificial intelligence framework (RAI) and could be used to guide decision-making authorities. The results show that the model accurately predicts the number of hospitalised cases, the longevity and the peaking points of the waves, which earns the trust of

Table A.1
The estimated parameters for each district in each wave.

District	Input parameter	Wave 1	Wave 2	Wave 3	Wave 4	Wave 5
	S_i starting value			$N_i - E_i - V_i$		
	E_{1i} starting value			1		
	I_{1i} starting value			0		
	I_{1i} starting value			0		
	I_{3i} starting value			0		
	I_{4i} starting value			0		
	R_i starting value			0		
	D_i starting value			0		
All	V_i starting value	0	$0.3N_i$	$0.4N_i$	$0.58N_i$	$0.9N_i$
	R_0			$\Gamma(57.2, 0.05)$		
	ρ			0.75		
	$\frac{1}{\sigma}$			$\Gamma(2,1)$		
	p_1			0.75		
	α_{23i}	0.002272727	0.003125	0.006	0.004	0.002
	α_{24i}	0.001282051	0.002083333	0.002173913	0.001612903	0.002380952
	g	0.80	0.67	0.67	0.67	0.67
	N			3522325		
	Ψ_i			19.67188339		
Tshwane	γ_{31}	$\Gamma(0.012, 8.035)$	$\Gamma(0.077, 1.296)$	$\Gamma(0.002, 61.717)$	$\Gamma(0, 46353.52)$	$\Gamma(0.001, 272.619)$
	γ_{41}	$\Gamma(0.012, 8.035)$	$\Gamma(0.077, 1.296)$	$\Gamma(0.002, 61.717)$	$\Gamma(0, 46353.52)$	$\Gamma(0.001, 272.619)$
	δ_{31}	$\Gamma(0.007, 3.164)$	$\Gamma(0.013, 1.339)$	$\Gamma(0.001, 10.255)$	$\Gamma(0.002, 67.534)$	$\Gamma(0.009, 0.202)$
	δ_{41}	$\Gamma(0.001, 49.589)$	$\Gamma(0.049, 1.288)$	$\Gamma(0.064, 0.891)$	$\Gamma(0.001, 5.805)$	$\Gamma(0.02, 1.352)$
	ν_i	$\Gamma(0, 0)$	$\Gamma(0.001, 0.156)$	$\Gamma(0.002, 0.575)$	$\Gamma(0.001, 1.213)$	$\Gamma(0.001, 0.646)$
	N			5538596		
	Ψ_i			15.36825768		
Johannesburg	γ_{32}	$\Gamma(0, 2139.376)$	$\Gamma(0.096, 1.506)$	$\Gamma(0, 1134.626)$	$\Gamma(0.01, 3.816)$	$\Gamma(0, 14704.91)$
	γ_{42}	$\Gamma(0.011, 7.655)$	$\Gamma(0.077, 1.272)$	$\Gamma(0.077, 1.272)$	$\Gamma(0, 12689.14)$	$\Gamma(0.003, 50.091)$
	δ_{32}	$\Gamma(0.001, 2.884)$	$\Gamma(0.004, 1.304)$	$\Gamma(0.004, 1.304)$	$\Gamma(0.002, 51.794)$	$\Gamma(0.003, 0.182)$
	δ_{42}	$\Gamma(0.001, 76.195)$	$\Gamma(0.05, 1.277)$	$\Gamma(0.05, 1.277)$	$\Gamma(0, 5.941)$	$\Gamma(0.054, 0.721)$
	ν_i	$\Gamma(0, 0)$	$\Gamma(0.001, 0.153)$	$\Gamma(0.003, 0.627)$	$\Gamma(0.003, 1.180)$	$\Gamma(0.001, 0.644)$
	N			3781377		
	Ψ_i			16.46564581		
Ekurhuleni	γ_{33}	$\Gamma(0, 42947.5)$	$\Gamma(0.105, 1.508)$	$\Gamma(0.105, 1.508)$	$\Gamma(0, 2.877)$	$\Gamma(0, 124948.9)$
	γ_{43}	$\Gamma(0.012, 7.869)$	$\Gamma(0.079, 1.297)$	$\Gamma(0.079, 1.297)$	$\Gamma(0, 52661.49)$	$\Gamma(0.001, 85.659)$
	δ_{33}	$\Gamma(0.003, 3.091)$	$\Gamma(0.003, 1.252)$	$\Gamma(0.003, 1.252)$	$\Gamma(0.02, 5.719)$	$\Gamma(0.002, 0.132)$
	δ_{43}	$\Gamma(0.001, 69.372)$	$\Gamma(0.047, 1.298)$	$\Gamma(0.047, 1.298)$	$\Gamma(0.001, 3.706)$	$\Gamma(0.014, 4.338)$
	ν_i	$\Gamma(0, 0)$	$\Gamma(0.001, 0.198)$	$\Gamma(0.002, 0.524)$	$\Gamma(0.001, 1.194)$	$\Gamma(0.001, 0.652)$
	γ_{34}	$\Gamma(0, 5618.201)$	$\Gamma(0.106, 1.508)$	$\Gamma(0.106, 1.508)$	$\Gamma(0.003, 15.411)$	$\Gamma(0, 15930.77)$
	γ_{44}	$\Gamma(0.022, 4.087)$	$\Gamma(0.079, 1.231)$	$\Gamma(0.079, 1.231)$	$\Gamma(0, 40739.05)$	$\Gamma(0.011, 10.557)$
	δ_{34}	$\Gamma(0.003, 3.336)$	$\Gamma(0.004, 1.379)$	$\Gamma(0.004, 1.379)$	$\Gamma(0.04, 3.431)$	$\Gamma(0, 0)$
Sedibeng	δ_{44}	$\Gamma(0.002, 44.392)$	$\Gamma(0.045, 1.438)$	$\Gamma(0.045, 1.438)$	$\Gamma(0.001, 1.211)$	$\Gamma(0, 0)$
	ν_i	$\Gamma(0, 0)$	$\Gamma(0.001, 0.184)$	$\Gamma(0.002, 0.532)$	$\Gamma(0.002, 1.156)$	$\Gamma(0.001, 0.660)$
	N			952102		
	Ψ_i			13.49495407		
	γ_{35}	$\Gamma(38.351, 0.002)$	$\Gamma(38.351, 0.002)$	$\Gamma(38.351, 0.002)$	$\Gamma(38.351, 0.002)$	$\Gamma(38.351, 0.002)$
	γ_{45}	$\Gamma(38.35, 0.002)$	$\Gamma(38.35, 0.002)$	$\Gamma(38.35, 0.002)$	$\Gamma(38.35, 0.002)$	$\Gamma(38.35, 0.002)$
West Rand	δ_{35}	$\Gamma(0.017, 0.204)$	$\Gamma(0.005, 1.279)$	$\Gamma(0.005, 1.279)$	$\Gamma(0, 0.242)$	$\Gamma(0, 0)$
	δ_{45}	$\Gamma(0.02, 3.879)$	$\Gamma(0.05, 1.476)$	$\Gamma(0.05, 1.476)$	$\Gamma(0, 0.406)$	$\Gamma(0.033, 0.775)$
	ν_i	$\Gamma(0, 0)$	$\Gamma(0.001, 0.185)$	$\Gamma(0.003, 0.430)$	$\Gamma(0.013, 0.793)$	$\Gamma(0.001, 0.625)$
	N			922640		
	Ψ_i			16.23844228		

health care and government decision-making authorities. The main challenge faced during the fitting of the model was the under-reporting of positive cases due to low testing rates, which mostly resulted in over-predicting mild cases. Under-reporting of positive cases underestimates the infectiousness and is a strong argument for why more attention should be given to test and tracing coverage in the future (Modisenyane et al., 2022). Other challenges when fitting the model were the COVID-19 variants that changed the transition rates over time. Future model approaches could extend this study and focus on estimating transition rates such as the as functions of time to capture disease transmission and severity variability. Additionally, the vaccination rate needs improvement by incorporating vaccination types and its efficiencies into the model. What the sensitivity analysis brought to light is that it is important to report how many tested cases were admitted to hospital. It is crucial to monitor this transition rate because it is the pivotal point of hospitals becoming overloaded. Comorbidity and age risks are also highlighted by the vaccination roll-out plan, which chose to vaccinate the elderly and people with comorbidities first. In the future, stigma and vaccine hesitancy could also be implemented in the model.

It is important to note that in the paper Fabris-Rotelli et al. (2022) on which this research is based, the reported data was at the ward level and not district level, due to limited data available at ward level in 2020. This high-resolution case data was not available in South Africa after 2020. The methodology for estimating the number of susceptible and vaccinated individuals during a pandemic is open to refinement and improvement. For example, the SEIRDV model can be improved by incorporating different vaccine scenarios, with the aim to optimise vaccination distribution using a spatial temporal vaccination policy. Our understanding of pandemic models has grown with the lessons learned from the COVID-19 experience. The methods used in this study are limited by the data available to us. This study was limited by the spatial resolution of district levels of Gauteng. Access to data at the ward level will provide data at a higher spatial resolution to better record the heterogeneity of each spatial area. This could pinpoint local breakouts accurately and strengthen control of the spread of the disease in a future study, should data be available. This study also comes to the same conclusion as the paper on population mobility (Potgieter et al., 2021), where the daily mobility was mostly identical, giving further grounds to improve the method to capture mobility changes at a higher spatial resolution in South Africa.

Overall, the study proved that immunity is the best defense weapon to have during a pandemic and that vaccinations gave overwhelming evidence that they protected many South Africans during the 4th and 5th waves of the pandemic. In conclusion, this study provides a useful model to guide decision-making authorities in their efforts to combat the spread of COVID-19.

Acknowledgements

Appendix. Estimates of each parameter of each wave

See Table A.1

References

Adam, D., 2020. Special report: The simulations driving the world's response to COVID-19.. Nature 580 (7802), 316–319.

Anderson, R., May, R., 1985. Vaccination and herd immunity to infectious diseases. Nature 318 (6044), 323–329.

Aràndiga, F., Baeza, A., Cordero-Carrión, I., Donat, R., Martí, M., Mulet, P., Yáñez, D., 2020. A spatial-temporal model for the evolution of the COVID-19 pandemic in Spain including mobility. Mathematics 8 (10), 1677.

Auchincloss, A., Gebreab, S., Mair, C., Diez Roux, A.V., 2012. A review of spatial methods in epidemiology, 2000–2010. Ann. Rev. Public Health 33, 107–122.

Baigent, S., McCauley, J., 2003. Influenza type A in humans, mammals and birds: Determinants of virus virulence, host-range and interspecies transmission. BioEssays 25 (7), 657–671.

Ben Chaouch, Z., Lo, A.W., Wong, C.H., 2022. Should we allocate more COVID-19 vaccine doses to non-vaccinated individuals? PLOS Glob. Public Health 2 (7), e0000498.

Cheng, Y., Tjaden, N., Jaeschke, A., Thomas, S., Beierkuhnlein, C., 2020. Deriving risk maps from epidemiological models of vector borne diseases: State-of-the-art and suggestions for best practice. Epidemics 100411.

Cohen, C., 2020. The Initial and Daily COVID-19 Effective Reproduction Number in South Africa. Tech. rep., The National Institute For Communicable Diseases.

Dhirasakdanon, T., Thieme, H., 2009. Persistence of vertically transmitted parasite strains which protect against more virulent horizontally transmitted strains. In: Modeling and Dynamics of Infectious Diseases. World Scientific, pp. 187–215.

Diggle, P., 2006. Spatio-temporal point processes: Methods and applications. Monogr. Statist. Appl. Probab. 107, 1.

Fabris-Rotelli, I., Holloway, J., Kimmie, Z., Archibald, S., Debba, P., Manjoo-Docrat, R., le Roux, A., Dudeni-Tlhone, N., van Rensburg, C.J., Thiede, R., Abdelatif, N., Potgieter, A., Makhanya, S., 2022. A spatial SEIR model for COVID-19 in South Africa. J. Data Sci. Stat. Vis.

Feng, Z., Towers, S., Yang, Y., 2011. Modeling the effects of vaccination and treatment on pandemic influenza. AAPS J. 13 (3), 427–437.

Fry, R., Hollinghurst, J., Stagg, H., Thompson, D., Fronterre, C., Orton, C., Lyons, R., Ford, D., Sheikh, A., Diggle, P., 2021. Real-time spatial health surveillance: Mapping the UK COVID-19 epidemic. Int. J. Med. Inform. 149, 104400.

Gnanvi, J., Salako, K., Kotanmi, G., Kakaï, R., 2021. On the reliability of predictions on COVID-19 dynamics: A systematic and critical review of modelling techniques. Infect. Dis. Model. 6, 258–272.

González, E., Villena, M., 2020. On the spatial dynamics of vaccination: A spatial SIRS-V model. Comput. Math. Appl. 80 (5), 733–743.

Hafeez, A., Ahmad, S., Siddqui, S., Ahmad, M., Mishra, S., 2020. A review of COVID-19 (Coronavirus Disease-2019) diagnosis, treatments and prevention. Eurasian J. Med. Oncol. 4 (2), 116–125.

Hindmarsh, A., 1982. ODEPACK, a systematized collection of ODE solvers. IMACS Trans. Sci. Comput. 1, 55–64.

Huang, C., Wang, Y., Li, X., Ren, L., Zhao, J., Hu, Y., Zhang, L., Fan, G., Xu, J., Gu, X., 2020. Clinical features of patients infected with 2019 novel coronavirus in Wuhan, China. Lancet 395 (10223), 497–506.

Jalilisadrabad, S., Zabetian Targhi, E., 2020. Investigating the location of organizational housing on the outskirts of cities (study sample: Accommodation of bandar abbas gas condensate refinery staff). Naqshejahan Basic Stud. New Technol. Archi. Planning 10 (1), 19–31.

Jewell, N., Lewnard, J., Jewell, B., 2020. Predictive mathematical models of the COVID-19 pandemic. JAMA 323 (19), 1893–1894.

Kong, L., Duan, M., Shi, J., Hong, J., Chang, Z., Zhang, Z., 2022. Compartmental structures used in modeling COVID-19: a scoping review. Infect. Dis. Poverty 11 (1), 1–9.

Kumar, A., Choi, T., Wamba, S.F., Gupta, S., Tan, K., 2021. Infection vulnerability stratification risk modelling of COVID-19 data: a deterministic SEIR epidemic model analysis. Ann. Oper. Res. 1–27.

le Roux, A., Cooper, A., Ludick, C., Arnold, K., Mans, G., 2021. Creating a set of high-resolution vulnerability indicators to support the disaster management response to the COVID-19 pandemic in South Africa. In: COVID-19 Pandemic, Geospatial Information, and Community Resilience. CRC Press, pp. 291–304.

Locatelli, I., Trächsel, B., Rousson, V., 2021. Estimating the basic reproduction number for COVID-19 in Western Europe. PLoS One 16 (3), e0248731.

Ma, Q., Gao, J., Zhang, W., Wang, L., Li, M., Shi, J., Zhai, Y., Sun, D., Wang, L., Chen, B., Jiang, S., Zhao, J., 2021. Spatio-temporal distribution characteristics of COVID-19 in China: A city-level modeling study. BMC Infect. Dis. 21 (1), 1–14.

Metcalf, T., Cubas, R., Ghneim, K., Cartwright, M., Van Grevenynghe, J., Richner, J., Olagnier, D., Wilkinson, P., Cameron, M., Park, B., Hiscott, J., Diamond, M., Wertheimer, A., Nikolich-Zugich, J., Haddad, E., 2015. Global analyses revealed age-related alterations in innate immune responses after stimulation of pathogen recognition receptors. Aging Cell 14 (3), 421–432.

Modisenyane, M., Madikezela, L., Mngemane, S., Ramadan, O., Matlala, M., McCarthy, K., Govender, N., Nemungadi, T., Silal, S., 2022. COVID-19 response in South African communities: Screening, testing, tracing and movement modelling. SAMJ 112 (5b), 366–370.

O'Brien, D.A., Clements, C.F., 2021. Early Warning Signals Predict Emergence of COVID-19 Waves. Cold Spring Harbor Laboratory Press, http://dx.doi.org/10.1101/2021.06.24.21259444, https://www.medrxiv.org/content/medrxiv/early/2021/06/26/2021.06.24.21259444.full.pdf.

Park, M., Cook, A., Tao, J., Sun, Y.L., Dickens, B., 2020. A systematic review of COVID-19 epidemiology based on current evidence. J. Clin. Med. 9 (4), 967.

Potgieter, A., Fabris-Rotelli, I., Kimmie, Z., Dudeni-Tlhone, N., Holloway, J., Janse Van Rensburg, C., Thiede, R., Debba, P., Docrat, N., Khuluse-Makhanyam, S., 2021. Modelling representative population mobility for COVID-19 spatial transmission in South Africa. Front. Big Data 4, 718351.

Shankar, S., Mohakuda, S.S., K.A., Nazneen, P., Yadav, A., Chatterjee, K., 2021. Systematic review of predictive mathematical models of COVID-19 epidemic. Med. J. Armed Forces India 77, S385–S392.

Silal, S.P., 2022. Seasonal targeting of the RTS, s/AS01 malaria vaccine: a complementary tool but sustained funding is required. Lancet Glob. Health 10 (12), e1693–e1694.

Silal, S., Groome, M., Govender, N., Pulliam, J., Ramadan, O., Puren, A., Jassat, W., Leonard, E., Moultrie, H., Meyer-Rath, K., et al., 2022. Leveraging epidemiology as a decision support tool during the COVID-19 epidemic in South Africa. SAMJ 112 (5b), 361–365.

Silal, S.P., Pulliam, J.R., Meyer-Rath, G., Jamieson, L., Nichols, B.E., Norman, J., Hounsell, R., Mayet, S., Kagoro, F., Moultrie, H., 2023. The national COVID-19 epi model (NCEM): Estimating cases, admissions and deaths for the first wave of COVID-19 in South Africa. PLOS Glob. Public Health 3 (4), e0001070.

Silal, S., Pulliam, J., Meyer-Rath, G., Nichols, B., Jamieson, L., Kimmie, Z., Moultrie, H., 2020. Estimating cases for COVID-19 in South Africa update: 19 May 2020. https://www.nicd.ac.za/wp-content/uploads/2020/05/SACMC_19052020_slides-for-MoH-media-briefing.pdf.

Smit, A., Fitchett, J., Engelbrecht, F., Scholes, R., Dzhivhuho, G., Sweijd, N., 2020. Winter is coming: A southern hemisphere perspective of the environmental drivers of SARS-CoV-2 and the potential seasonality of COVID-19. Int. J. Environ. Res. Public Health 17 (16), 5634.

Thiede, R., Abdelatif, N., Fabris-Rotelli, I., Manjoo-Docrat, R., Holloway, J., Janse van Rensburg, C., Debba, P., Dudeni-Tlhone, N., Kimmie, Z., le Roux, A., 2020. Spatial variation in the basic reproduction number of COVID-19: A systematic review. arXiv preprint arXiv:2012.06301.

Turok, I., Visagie, J., Scheba, A., 2021. Social inequality and spatial segregation in Cape Town. In: Urban Socio-EConomic Segregation and Income Inequality. Springer, Cham, pp. 71–90.

Wang, J., Jing, R., Lai, H., Lyu, Y., Knoll, M., Fang, H., 2020. Acceptance of COVID-19 vaccination during the COVID-19 pandemic in China. Vaccines 8 (3), 482.

Whitty, C., 2015. What makes an academic paper useful for health policy? BMC Med. 13 (1), 1–5.

Woolf, S., Joubert, J., 2013. A people-centred view on paratransit in South Africa. Cities 35, 284–293.

Woolf, S., Joubert, J., 2014. A Look at Paratransit in South Africa. Tech. rep., University of Pretoria, South Africa.

World Health Organisation, 2023. Estimating cases for COVID-19 in South Africa. Assessment of alternative scenarios, https://www.who.int/publications/m/item/draft-landscape-of-COVID-19-candidate-vaccines,

Zhou, S., Zhou, S., Zheng, Z., Lu, J., 2021. Optimizing Spatial Allocation of COVID-19 Vaccine by Agent-Based Spatiotemporal Simulations, GeoHealth, e2021GH000427.